Superhydrophobic surfaces: A model approach to predict contact angle and surface energy of soil particles

J. BACHMANN[a] & G. McHALE[b]

[a] *Institute of Soil Science, Leibniz University Hannover, Herrenhaeuser Str.2, 30419, Hannover, Germany*

[b] *School of Science & Technology, Nottingham Trent University, Clifton Lane, Nottingham, NG11 8NS, UK.*

Contacts: Jörg Bachmann. Email: bachmann@ifbk.uni-hannover.de

Glen McHale. Email : glen.mchale@ntu.ac.uk

Abstract

Wettability of soil affects a wide variety of processes including infiltration, preferential flow and surface runoff. The problem of determining contact angles and surface energy of powders, such as soil particles, remains unsolved. So far, several theories and approaches have been proposed, but formulation of surface and interfacial free energy, as regards its components, is still a very debatable issue. In the present study, the general problem of the interpretation of contact angles and surface free energy on chemically heterogeneous and rough soil particle surfaces are evaluated by a reformulation of the Cassie-Baxter equation assuming that the particles are attached on to a plane and rigid surface. Compared with common approaches, our model considers a roughness factor which depends on the Young's Law contact angle determined by the surface chemistry. Results of the model are discussed and compared with independent contact angle measurements using the Sessile Drop and the Wilhelmy Plate methods. Based on contact angle data, the critical surface tension of the grains were determined by the method proposed by Zisman. Experiments were made with glass beads and three soil materials ranging from sand to clay. Soil particles were coated with different loadings of dichlorodimethylsilane (DCDMS) to vary the wettability. Varying the solid surface tension using DCDMS treatments provided pure water wetting behaviours ranging from wettable to extremely hydrophobic with contact angles >150°. Results showed that the critical surface energy measured on grains with the highest DCDMS loadings was similar to the surface energy measured independently on ideal DCDMS -coated smooth glass plates, except for the clay soil. Contact angles measured on plane surfaces were related to contact angles measured on rough grain surfaces using the new model based on the combined Cassie-Baxter Wenzel equation which takes into account the particle packing density on the sample surface.

Introduction

The wetting behaviour of an ideal flat surface is determined by its chemical composition and the molecular properties of the wetting liquid. Soils are, in general, characterized by extremely large surface to volume ratios and surfaces formed by soil are far from flat. Basic interfacial properties of mineral soils, such as the surface charge density, polarity, specific surface area etc., may therefore significantly influence swelling and shrinkage, water sorption and permeability or adsorption of colloids and molecules from soil solution in bulk soil. Contact angles (CA) are influenced to a marked extent by physicochemical characteristics such as structural arrangement of surface functional groups and surface charge density of the solid-liquid interface. As a result, they are, in principle, sensitive to physical and chemical modifications of the substrate. The large sensitivity of the contact angle is widely used to control the wetting process of surfaces. As a consequence, contact angles provide a sensitive means for analysis of interfaces conditioned with materials adsorbed from soil solution or formed directly on grain surfaces. Naturally occurring water repellency of soil is generally attributed to organic soil components (Roberts & Carbon, 1972). The organic matter may either cover the mineral grains as thin coatings or exist as adsorbed nano-scaled microaggregates (Bachmann *et al.*, 2008). If hydrophobic substances at the solid surface are combined with a rough surface structure, a water drop deposited on a surface can remain almost spherical (Neinhuis & Barthlot, 1997). For example, Feng *et al.* (2002) used a combination of roughness scales by combining the Cassie-Baxter equation for large pillars with Wenzel´s equation for the lower-scale roughness on top of the peaks. They produced structures with micro- and nano-roughness displaying a high contact angle when the surface chemistry itself was hydrophobic. McHale *et al.* (2005, 2007), have recently suggested that Cassie-Baxter and Wenzel concepts may also be applicable to surfaces formed by soil particles.

Determination of the wettability of a surface composed of soils and how it depends separately on the roughness and the surface chemistry presents significant challenges. Soil particles are generally rough, irregularly shaped, chemically heterogeneous and non-rigid, and, in some cases such as with clay, swell when placed in contact with water. Moreover, in the capillary rise method (CRM), which has commonly been applied to soil particles (Siebold *et al.*, 1997; Goebel *et al.*, 2004), the time of contact between liquid and soil particles depends on the contact angle itself. Recent work by Marmur (2003) and Lavi *et al.* (2008) showed that contact angles for certain combinations of pore radius and viscosity of the test liquids can be considerably in error through effects caused by inertia, friction (Stange *et al.*, 2003) and the dynamic contact angle (Lavi *et al.*, 2007), which are in practice not considered when standard procedures (e.g. Siebold *et al.*, 1997) to evaluate the contact angle are applied. The contact angle determined from the initial capillary rise process evaluated with the conventional Lucas-Washburn equation are in many cases too large compared with the equilibrium contact angle. As a consequence, the solid surface free energy components calculated via such overestimated contact angles are significantly smaller than those obtained from contact angles measured directly on ideal surfaces. Further, effects such as pore topology may affect the capillary rise of water and the wetting reference liquid differently. Therefore, the main objectives of the present paper are i) to determine the critical surface energy γ_C of ideal and rough surfaces, respectively, and ii) to confirm whether the model used in the present paper is

able to convert contact angles measured on ideal smooth surfaces to contact angles measured on rough surfaces.

We first review a simple model, which uses an analysis in the changes of surface free energy to describe the equilibrium contact angle on complex heterogeneous surfaces. The surface considered consists of a set of rough surface protrusions into which the liquid completely penetrates (Wenzel-like), but with the liquid bridging between these surface protrusions (Cassie-like). The results of the model are then used to predict the observed contact angle for a set of equally distributed spherical grains, as a model of a set of soil particles affixed to a plate. To compare the results of this model with independent experimental measurements, we propose simple techniques to measure the initial contact angle of rough particle surfaces with two methods adapted to soil particles (Bachmann *et al*., 2003). The first technique is the Wilhelmy Plate Method (WPM) (Wilhelmy, 1863), which has recently been applied for soil material (e.g. Bachmann *et al*., 2003) and which has the advantage of yielding retreating angle results just as easily as advancing angles. The second technique is the Sessile Drop Method (SDM) for drops with an infinite size (Good, 1993); the recorded data should correspond under ideal conditions (smooth and homogeneous surfaces). Thus, we are able to discuss and compare results from model calculations with contact angle data measured with two different methods on surfaces with increasing degrees of roughness from smooth to extreme complex surface topography.

Theory

First principles derivation of the equilibrium contact angle

On smooth and chemically heterogeneous planar surfaces, two approaches to the equilibrium contact angle, θ_e^Y, exist: force balance and minimum surface energy. In the force approach the interfacial tensions, γ_{ij}, where the subscripts i and j may take the values S, L and V representing the solid, liquid and vapour phases, are regarded as forces per unit length and a horizontal force balance at the contact line is imposed: $\gamma_{SL} + \gamma_{LV}\cos\theta_e^Y = \gamma_{SV}$. In the energy approach, the interfacial tensions, γ_{ij}, are regarded as energies per unit area and the energy change due to a small displacement of the liquid-vapor interface is assumed to vanish. Either approach gives rise to the Young equation (Equation1) (Young, 1805):

$$\cos\theta_e^Y = (\gamma_{SV} - \gamma_{SL})/\gamma_{LV} \qquad (1)$$

On heterogeneous surfaces, problems can arise with the force view, because the surface may be continuous, but non-differentiable thus preventing a simple resolving of forces. In contrast, the energy view provides a simple approach to surfaces that are patterned or rough, irrespective of whether the patterning is chemical or topographic. To derive the surface energy of a composite rough and structured surface from first principles, the surface energy change, ΔF, caused by a displacement, ΔA, of the contact line has to be considered.

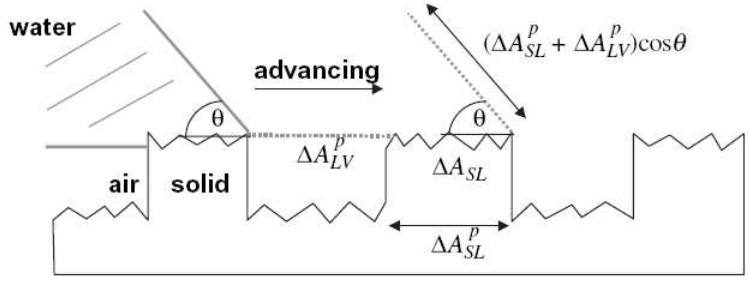

Figure 1 Equilibrium contact angle from minimum surface free energy for rough surface with both Cassie-Baxter and Wenzel affects.

Figure 1 shows a schematic diagram of a surface consisting of surface protrusions which themselves are rough. In this derivation, it is assumed that an advancing liquid front bridges between the surface features, but that the liquid fully penetrates the roughness at the top of the features. In this situation, the small advance of the liquid front indicated in Figure 1 creates an additional liquid-vapour surface area, ΔA^p_{LV}, as it bridges the gap to the next surface feature, and an additional solid-liquid interfacial area, ΔA_{SL}. Because the liquid is assumed to penetrate into the rough surface at the top of each protrusion, the true area is related to the planar projection of the surface by $\Delta A_{SL} = r_g \Delta A^p_{SL}$, where r_g is the Wenzel roughness factor; in these equations the superscript p signifies planar areas. The advancing liquid also creates an additional liquid-vapour area because of the additional area of the meniscus of $(\Delta A^p_{LV}+\Delta A^p_{SL})\cos\theta$, where θ is the contact angle (Figure 1). Scaling these changes in interfacial area by the corresponding interfacial energies per unit area gives a total change in surface free energy of:

$$\Delta F = \Delta A^p_{LV}\gamma_{LV} + \Delta A_{SL}(\gamma_{SL} - \gamma_{SV}) + (\Delta A^p_{SL} + \Delta A^p_{LV})\gamma_{LV}\cos\theta \qquad (2)$$

Defining $\Delta A^p_T = \Delta A^p_{SL} + \Delta A^p_{LV}$ and $\cos\theta^Y_e = (\gamma_{SV} - \gamma_{SL})/\gamma_{LV}$ (Young´s law), Eq. 2 can be rewritten as:

$$\frac{\Delta F}{\gamma_{LV}\Delta A^p_T} = \frac{\Delta A^p_{LV}}{\Delta A^p_T} - \frac{\Delta A^p_{SL}}{\Delta A^p_T} r_g \cos\theta^Y_e + \cos\theta \qquad (3)$$

where the earlier definition of the Wenzel roughness factor, $r_g=\Delta A_{SL}/\Delta A^p_{SL}$, has been used. For equilibrium, this energy change of ΔF, given by Eq. 3, must vanish when the contact angle, θ, is at its equilibrium value, θ_e^{net}, thus giving:

$$\cos\theta^{net}_e = \frac{\Delta A^p_{SL}}{\Delta A^p_T} r_g \cos\theta^Y_e - \frac{\Delta A^p_{LV}}{\Delta A^p_T} \qquad (4)$$

By defining a Cassie solid fraction, φ_s, using $\Delta A^p_{SL} = \varphi_s \Delta A^p_T$, and noting that $\Delta A^p_{LV}=\Delta A^p_T - \Delta A^p_{SL}$, Eq. 4 can be written as:

$$\cos\theta^{net}_e = \varphi_S r_g \cos\theta^Y_e - (1-\varphi_S) \qquad (5)$$

Recognising that the Wenzel contact angle, θ_W, is defined by:

$$\cos\theta_W = r_g \cos\theta_e^Y \tag{6}$$

and then gives the key relationship:

$$\cos\theta_e^{net} = \varphi_S \cos\theta_W - (1-\varphi_S) \tag{7}$$

Thus, the observed contact angle, θ_e^{net}, on this composite surface involving the liquid completely following the surface roughness at the tops of features, but then bridging between features, is a modified Cassie-Baxter equation in which the Wenzel contact angle, θ_W, is used in place of the usual Young's Law contact angle, θ_e^Y. Intuitively, this result can be interpreted as resulting from the surface roughness first transforming the Young's Law contact angle to the Wenzel contact angle, followed by the bridging effect transforming the Wenzel contact angle via a Cassie-Baxter equation, i.e.

$$\theta_e^Y \xrightarrow{Wenzel} \theta_W \xrightarrow{Cassie-Baxter} \theta_{CB}$$

Derivation of a 'soil model'

The previously derived results can be applied to a layer of spherical particles modelling a set of soil grains. Figure 2a shows the side view of the liquid as it bridges the spheres and considers the change in surface free energy that would result from an effective advance of the contact line by one period of the system; Figure 2b shows the relationship between the wetted portion of a sphere and the planar projection for the wetted area. Since the liquid retains complete contact with a portion of each sphere, the curvature of the solid results in a solid-liquid contact area that is greater than its planar projection, thus giving a roughness factor and, hence, a Wenzel effect. The liquid also bridges between neighbouring spheres and so provides, additionally, the Cassie-Baxter effect. This can be seen from the side-view in Figure 2a and also from the top view in Figure 2c, which shows the contact of the liquid with a set of spheres arranged in a triangular lattice and where each have a spherical radius, R, and centre-to-centre separation $2(1+\varepsilon)R$. The ε parameter allows the effective particle separation to be varied; a non-zero value of ε ensures that the spheres are arranged such that they are non-contacting. Since both the true area of liquid contact on a given sphere is larger than the planar projection of the area and a bridging of the air gap between spheres exists, there is a combined Wenzel roughness and Cassie-Baxter solid fraction effect and Eq. 7 therefore applies to this system. One important difference to the previous section is that the ratio of surface areas defining the roughness, $r_g=\Delta A_{SL}/\Delta A^p_{SL}$, now depends on how far down a sphere the liquid contacts and this itself depends on the Young's Law contact angle θ_e^Y. Thus, r_g is no longer a global property of the surface, but depends on the liquid used (McHale, 2007); the Cassie solid fraction, φ_s, also depends on the liquid used.

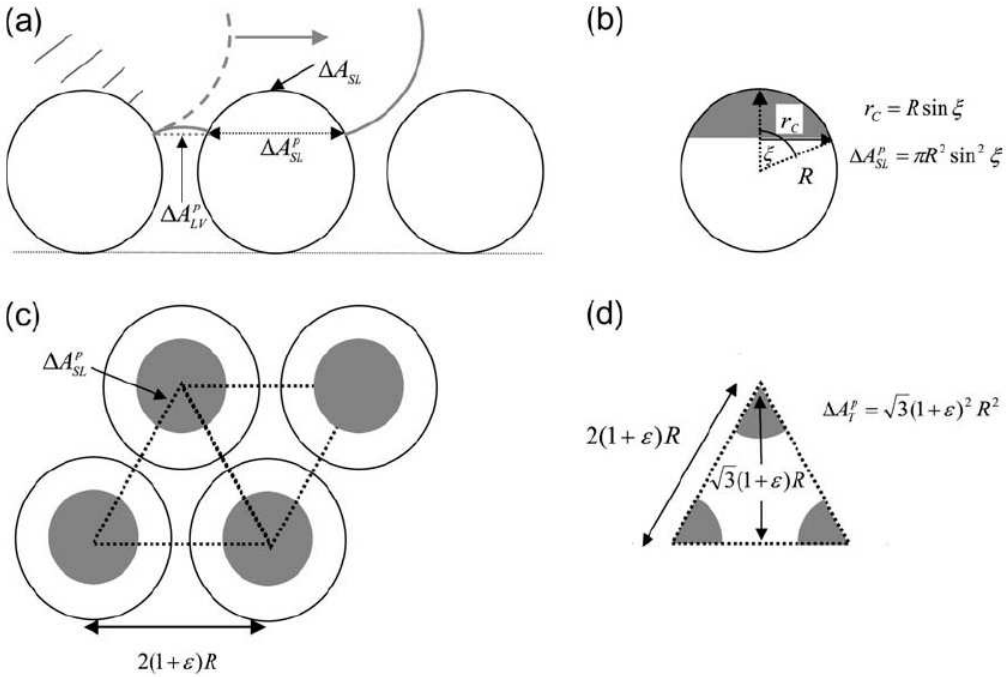

Figure 2 Geometry of the soil model for (a) side view, (b) relationship of parameters to wetted area on a sphere, (c) top view and (d) elementary cell for calculations.

Using Figure 2, trigonometry can be used to calculate the various areas required to estimate the roughness and Cassie fractions needed for evaluating Equation 7. The basic approach for calculating the solid-liquid contact area and its planar projection is to consider as an elementary cell the equilateral triangle shape that joins the centres of the tops of three adjacent spheres (Figure 2d). The planar projection of liquid-solid contact area within the triangle is $\Delta A_{SL}^{P}=½\ \pi r_c^2=½\ \pi R^2\sin^2\xi$, where r_c and ξ are the planar radius and the angle defined by Figure 2b and $\xi=\pi-\theta$. Since the actual area of solid-liquid contact on any one sphere is $2\pi R^2(1-\cos\xi)$, the total area of solid-liquid contact for the tops of the spheres within the area indicated by the triangle is $\Delta A_{SL}=\pi R^2(1-\cos\xi)$. In these areas, the angle ξ is determined by the Young's Law contact angle and, noting that $\sin\xi=\sin\theta_e^{Y}$ and $\cos\xi=-\cos\theta_e^{Y}$, gives $\Delta A_{SL}^{P}=½\ \pi R^2\sin^2\theta_e^{Y}$ and $\Delta A_{SL}=\pi R^2(1+\cos\ \theta_e^{Y})$. Thus, the Young's Law contact angle dependent Wenzel roughness factor can be evaluated as:

$$r_g = \frac{2(1+\cos\theta_e^{Y})}{\sin^2\theta_e^{Y}} \tag{8}$$

We note that although this roughness factor tends to infinity when θ_e^{Y} tends to zero, the combination of the roughness factor multiplied by the planar projection of the solid-liquid area (i.e. $r_g\Delta A_{SL}^{P}$) tends to a constant equal to half the surface area of a sphere (the factor of one-half is because we are considering the three sector areas in the triangle in Figure 2d). One subtlety is that for $\theta_e^{Y}<90^o$ a spherical surface behaves as a re-entrant surface (i.e. it curves in under itself). In this situation, the planar projection of solid-liquid area on a sphere, as defined for use in Equation 2, is then determined by the non-wetted area defined by the closure of the contact line and this tends to zero as θ_e^{Y} tends to zero.

The final area required for use with Equation 7 is the total planar area within the unit cell and this is given by the area of the equilateral triangle, which is $\Delta A^p_T = \sqrt{3}\,(1+\varepsilon)^2 R^2$. The Young's Law dependent Cassie solid fraction defined by $\varphi_s = \Delta A^p_{SL}/\Delta A^p_T$, is then:

$$\varphi_s = \frac{\pi \sin^2 \theta_e^Y}{2\sqrt{3}(1+\varepsilon)^2} \tag{9}$$

Using these parameterizations for Eq.7 leads to:

$$\cos\theta_e^{net} = \frac{\pi(1+\cos\theta_e^Y)}{\sqrt{3}(1+\varepsilon)^2}\cos\theta_e^Y - \left(1 - \frac{\pi \sin^2 \theta_e^Y)}{2\sqrt{3}(1+\varepsilon)^2}\right) \tag{10}$$

This equation is different to the result published by McHale *et al.* (2005) using a similar model of spherical spheres, but in which the Cassie solid fraction was defined by using $\Delta A_{SL} = \varphi_s(\Delta A_{SV} + \Delta A_{LV})$ and then implemented in the usual Cassie-Baxter equation. In the present case, Equation 10 is a direct result of the derivation, from first principles, of Equation 7. The effect of varying the liquid-gas interface with θ_e^Y is much stronger in the current model (Equation10) than previously predicted. We note that when the right hand side of Equation. 10 predicts $\cos\theta_e^{net} > 1$, it indicates that a situation of complete wetting has been achieved and, strictly speaking, no equilibrium contact angle exists. In the following section, we compare the model calculations of the average surface energy of a rough and composite surface with surface free energy calculations based on independent contact angle measurements obtained using the Wilhelmy Plate Method as described by Bachmann *et al.* (2003).

Materials and methods

Samples and test liquids

Regular glass slides (2.5 x 7.5 cm, average composition: SiO_2= 73.5 %, Na_2O = 15 %, CaO = 5.4 %, and MgO = 4.4 %; MENZEL, Braunschweig, Germany*)* and soil particles, respectively, were coated with dichlorodimethylsilane (DCDMS) and used as ideal and rough surfaces for the CA determination as a function of the liquid surface tension, γ_{LV}. Solid glass beads (SWARCO Vestglas GmbH, Germany) of 40-70 µm size fraction were used as ideal model systems having uniform spherical particles with a low degree of visible surface roughness. To compare the results from model surfaces with irregular shaped particles three wettable soils, extremely different in particle size, shape and particle size distribution (see Table 1), were made hydrophobic in the laboratory by coating the surfaces with different amounts of DCDMS. Based upon soil texture, the amount of applied DCDMS for beads and soils varied between 0.02 to 32 ml per 100 g (Table 2). This procedure provided material that retains non-biodegradable hydrophobicity after 180 days in contact with water (Bachmann *et al*., 2001). Bachmann *et al*. (2006) have shown that the largest dose of DCDMS, used in this study, was sufficient to increase the CA for water up to a constant maximal value. Sample preparation was performed by covering glass plates on both sides with double sided adhesive tape and then sprinkling particles onto the tape where they became fixed (Figure 3 and 4). The photograph in Figure 3 shows a relatively dense layer of particles, although on average the particles were not close-packed, indicating $\varepsilon > 0$.

Table 1 Proportions of particles (wt %) in various size fractions (in µm) of soil samples and glass beads.

Soil	Sand 630-2000	Sand 200-630	Sand 63-200	Silt 20-63	Silt 6.3-20	Silt 2-6.3	Clay <2 µm
White Sand	1.08 ± 0.07	93.84 ±0.29	5.38 ± 0.37	0.21 ±1.43	0.21 ± 0.58	0.42 ± 0.32	0.12 ± 0.16
Clay Loam	5.00 ± 0.86	14.89 ±0.48	12.27 ± 1.10	16.72 ±0.59	15.16 ±0.93	6.06 ± 0.32	29.89 ±0.41
Clarinda Clay	0.59 ± 0.00	3.11 ± 0.09	2.97 ± 0.06	14.05 ±1.41	15.70 ±0.93	4.75 ± 0.38	58.83 ±0.70
Glass Beads	0	0	0.11±0.16	69.18±1.27	30.72±1.31	0	0

Table : Selected soil properties and doses of DCDMS applied to samples. C_{total} is total carbon content, C_{org} the organic carbon content.

Soil	C_{total}	C_{org}	$CaCO_3$	SSA* m^2/g	Amount of DCDMS added [ml / 100 g]					
					0	I	II	III	IV	V
White Sand	0	0	0	0.01	0.00	0.02	0.12	0.24	0.48	0.96
Clay Loam	1.32	0.01	0.10	4.35	0.00	1.05	2.10	4.20	8.40	16,80
Clarinda Clay	1.04	1.04	0	30.00	0.00	1.05	2.10	4.20	8.40	33,60
Glass Beads	-	-	-	0.07	0.00	0.12	0.24	-	-	-

* Specific surface area, measured by BET - N_2 adsorption.

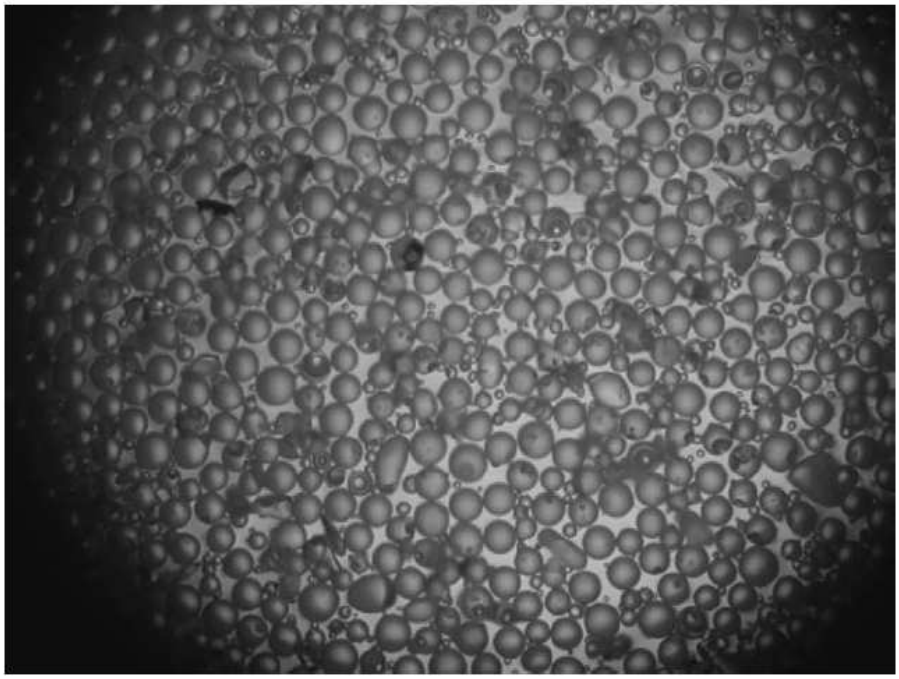

Figure 3 Example image of a layer of glass beads (40-70 µm) formed on double sided tape attached to a glass slide, used for contact angle measurement by sessile drop (SDM) and Wilhelmy plate (WPM) methods.

The Scanning Electron Microscope images in Figure 4 show sample surfaces prepared from soil with a non-uniform particle size distribution. Figure 4 shows a dense layer of different sized particles, no matter whether coarse sand fraction or mainly the clay fraction is attached. Figure 4 also shows the different shape of the particles ranging from almost spherical for the sand to an irregular platy structure for the clay particles. In our study, three to four plates of each soil were investigated; for more details see Bachmann *et al*. (2000).

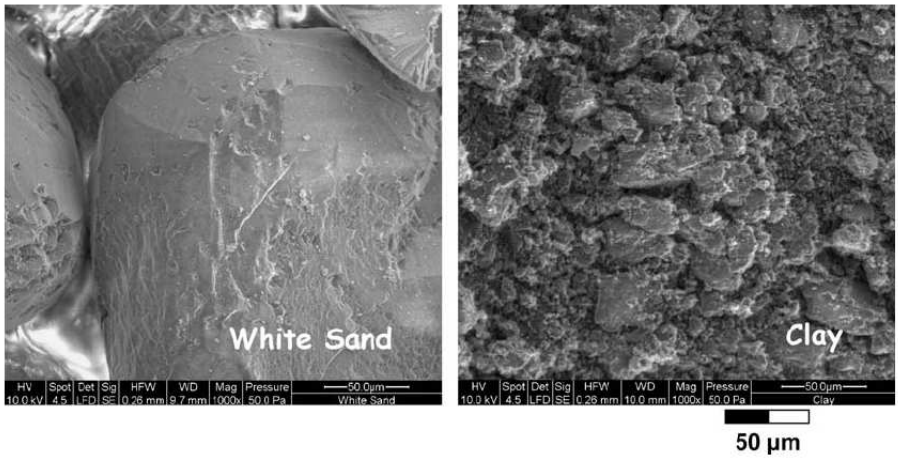

Figure 4 SEM images of white sand and (Clarinda) clay particle layer mounted on glass slides using double sided adhesive tape and typical of specimens used to determine contact angles by sessile drop (SDM) and Wilhelmy plate (WPM) methods.

Test liquids with defined liquid surface tensions, γ_{LV}, were produced by mixing water and ethanol from pure water (0%; γ_{LV} = 71.9 mJ m^{-2}) to 96% ethanol (γ_{LV} = 23 mJ m^{-2}). The data were fitted with a regression model (with $r^2 > 0.98$) using $\gamma_{LV} = a \cdot e^{-b \cdot E} + c \cdot e^{-d \cdot E}$, where E is the ethanol concentration in percent by volume, a=35.4703, b=0.0871, c=37.2692 and d=0.004986. The liquid surface tension was measured with the tensiometer directly after the CA determination for approximately 40% of all WPM measurements. The surface tension of the liquid in the reservoir used for the WPM measurements showed no evidence of contamination from the samples. In general, changes in γ_{LV} before and after the CA measurement were less than 1-2 mJ m^{-2}, indicating that the temporary contact between sample surface and testing liquid during immersion did not alter the sample surface through selective dissolution of components either dissolved from the tape or from the sample itself.

Contact angle measurement and analysis

The Wilhelmy plate method is a standard method to assess either surface tensions of unknown liquids or the CA on smooth surfaces. Theoretically, the WPM allows the determination of contact angles in the range from 0° to 180°. In recent investigations, the method has also been applied to rough or chemically heterogeneous samples (Bachmann *et al*., 2003; Arye *et al*., 2006; Bachmann *et al*., 2006). The method (Wilhelmy, 1863) enables assessment of dynamic advancing, θ_a, or receding contact angles, θ_r, by gradually immersing the sample to a prescribed depth in a test liquid and then subsequently withdrawing it. A schematic representation of the method adapted to soil particles and the governing equations to calculate the contact angle has been presented by Bachmann *et al*. (2003). Measurements of advancing and receding contact angles were made with a precision tensiometer (DCAT 11, DATA PHYSICS, Germany). Immersion and withdrawal speed were varied between 1 and 10^{-3} mm s^{-1}. Stable advancing and receding contact angles (θ_a and θ_r) were observed for speeds below

0.2 mm s^{-1} (Bachmann *et al*., 2006). With known γ_{LV}, the Wilhelmy Plate Method contact angle θ can be measured by using:

$$\cos\theta = F/(p\gamma_{LV}) \tag{11}$$

where F is the force (weight of the sample in air assessed by the balance) and p is the perimeter of the sample (wetted length). In our study, the equilibrium values of Wilhelmy Plate Method contact angles (WPM-CA), on rough surfaces, were determined by averaging the cosines of θ_a and θ_r according to Marmur (1994):

$$\theta_e^{net} = \arccos[(\cos\theta_a + \cos\theta_r)/2] \tag{12}$$

Sessile drop method contact angle measurements (SDM-CA) were made with a goniometer scale fitted microscope (Bachmann *et al*., 2000). Readings were taken at the three-phase contact line. Accuracy of the measurements was approximately ±2.5° within the range of 10°-170°. Readings of the angles on the silanized glass plate (5 drops, 10 readings per sample) were performed twice. All measurements were performed at a relative humidity of 50-65% in the laboratory. Water drops of volume 2 µl were placed on the sample surface using a microsyringe and, within 40 seconds, 10 replicate contact angle measurements were taken. The SDM-CA measured on the smooth glass plate was considered as the equilibrium contact angle, θ_e^Y, and the SDM-CA measured on rough samples was considered as the equilibrium value, θ_e^{net}, for comparison with values obtained with the WPM-CA.

Data pairs of the measured contact angle, θ, and corresponding surface tension, γ_{LV}, of various liquids are often used to estimate the surface tension of the dry solid surfaces. Preliminary experiments show (Bachmann *et al*. 2003; Arye *et al*, 2006) that for soil particles an ethanol mixture series produced a reproducible and linear relation for $\cos\theta = f(\gamma_{LV})$ for θ <90°, as proposed by Zisman (1964):

$$\cos\theta = b_0 + b_1\gamma_{LV} \tag{13}$$

where b_o and b_1 are empirical fitting parameters. The equality between γ_{LV} and γ_C is conceptual entity given for a contact angle of zero degrees, i.e. $\cos\theta = 1$, which defines γ_C as:

$$\gamma_C \coloneqq \gamma_{LV} \cong \gamma_{SV} \tag{14}$$

where γ_C is the critical surface energy or tension of the solid surface and is related to the surface free energy of the solid (Zisman, 1964). This approach is often used (Spelt & Neumann, 1992) but should be considered as semi-empirical, in particular for heterogeneous and rough solid surfaces. In general, different groups of liquids, i.e alcohols or hydrocarbons, provide linear relations but slightly different critical surface energies γ_C (Spelt & Neumann, 1992). For two liquids on a solid, the approximation may often be made that adsorption at the two liquid-solid interfaces is negligible, but this assumption is seldom tested directly. However, when using soil particles, many investigators have confirmed the general advantage of this approach compared with the use of pure organic liquids; this might be explained by the

fact that soil is generally a poorly-defined mixture of many organic and inorganic components.

Results and discussion

We determined the critical surface tension for DCDMS coatings on ideal glass surfaces by analysing the SDM and mean WPM-CA as a function of the liquid surface tension γ_{LV} (Figure 5).

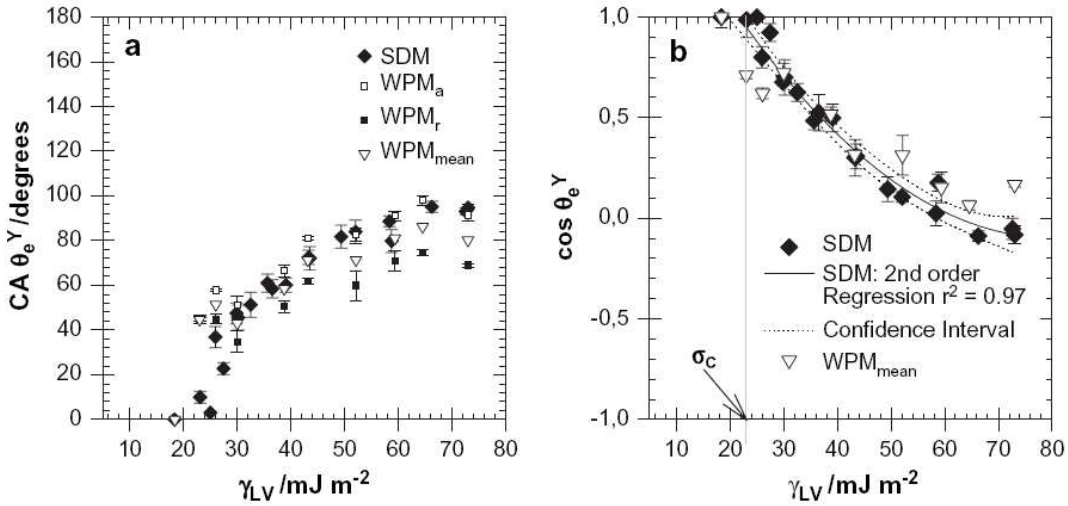

Figure 5 Sessile Drop and Wilhelmy Plate contact angles as a function of the liquid surface tension on a smooth hydrophobized glass plate (a). (b) shows the corresponding Zisman Plots. The vertical line shows the critical surface energy γ_C of the solid.

Sessile drop contact angles θ_e^Y for water (γ_{LV}=72 mJ m^{-2}) were around 90°, which were similar with the mean WPM-CA. As γ_{LV} decreased with increasing ethanol concentrations, decrease of CA to 0° was observed with both methods, but there were some notable differences between them. The CA obtained from the WPM is essentially a value averaged over the wetted perimeter of the solid, thus providing sampling of a much larger area of solid compared with the SDM. Although this should improve the precision of the measurement, this was not observed. Generally, the maximum observed SDM contact angle falls within θ_a and θ_r of the dynamic CA range of the WPM, but nearer to θ_a (Good, 1993). The present data (Figure 5) indicate that SDM-CAs were slightly larger than average WPM-CAs. Data from the literature indicate that the equilibrium CA can, in principle be estimated from CA hysteresis data (Kamusewitz *et al*., 1999; Meiron *et al*., 2004). Our results suggest that the SDM-CA is slightly larger than equilibrium CA averaged from the advancing and receding WPM-CAs. Transition of the CAs to zero was observed for the SDM between γ_C = (25 ± 2) mJ m^{-2} and slightly below this for WPM. This indicates that the critical surface energy of the smooth glass plate was slightly method-independent and was close to the value proposed for DCDMS coated glass surfaces (Zisman, 1964).

Arrangements of similarly shaped, uniformly sized particles supported on smooth glass plates present complex surfaces. Wenzel´s equation is of particular interest here, because it predicts that equilibrium wetting behaviour induced by surface chemistry can be modified by topography. As the dose of DCDMS increased, the CAs of all rough arrangements of particles increased irrespective of the ethanol concentration. Contact angles and CA hysteresis for samples subjected to the highest dose of DCDMS increased with

increasing γ_{LV} (Figure 6). According to Good (1993), a greater hysteresis between advancing and receding CA indicates greater chemical heterogeneity of the surface as shown in Figure 6 compared with the glass plate (Figure 5). Tschapek (1984) found that humic acids originating from soil always possess hydrophobic and hydrophilic sites, no matter how hydrophobic the surfaces are, and this implies CA hysteresis for soil materials. Enhancement of CA hysteresis is also a consequence of the Wenzel effect (McHale *et al.*, 2004). The combination of the hydrophobic surface chemistry and the increased surface area provided by an arrangement of smooth spheres in comparison with a plane surface, leads through Cassie-Baxter air-bridging to a superhydrophobic system. However, any effect of this, when the CA obtained from the SDM was >150° was not observed with any of the specimens tested.

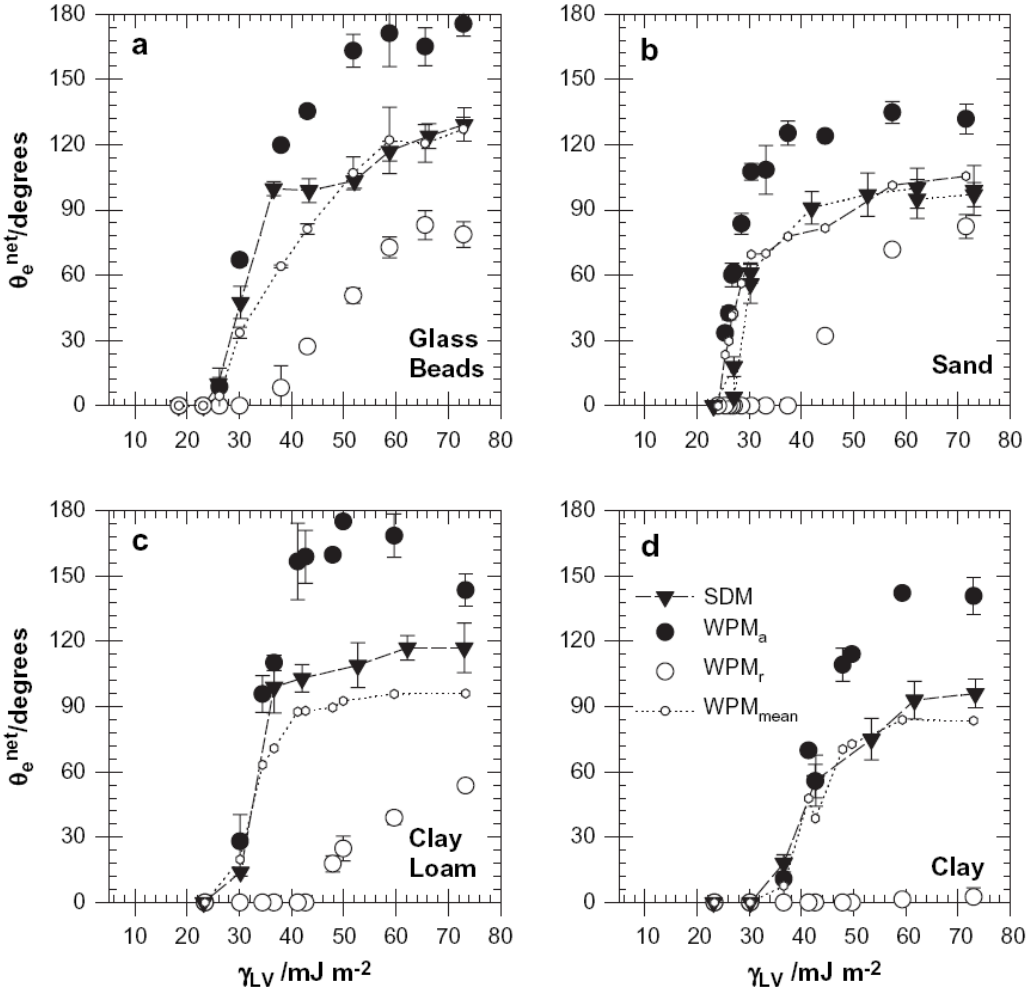

Figure 6 Sessile Drop and Wilhelmy Plate contact angles (advancing, receding and mean contact angle) as a function of liquid surface tension for glass beads (a) and three soil materials (b-d) for the maximum dichlorodimethylsilane dose.

Relatively good agreement was obtained between the average WPM-CA and that of the SDM (Figure 6b-d), except for the clay loam soil, which possessed the most non-uniform texture. This supports the hypothesis that the average WPM-CA represents the apparent equilibrium CA θ_e^{net} on rough surfaces, approximated by the SDM-CA. This also suggests that the estimation of the sample perimeter (essential for correct WPM-CA determination) derived from macroscopic measurements, which neglects the detailed tortuosity of the three phase boundary line, is appropriate.

Wenzel's equation predicts that for θ_e^Y > 90°, the effect of roughness is to increase the contact angle towards 180° and for θ_e^Y < 90° to decrease it towards 0°. This soil surface model predicts enhanced water repellency by particles whose surface chemistry has θ_e^Y > 90°. If the surface chemistry has θ_e^Y <90°, it is less water repellent, when the distance between particles is ~< 30% of the particle radius. Compared with other approaches (e.g. McHale & Newton, 2002), our model considers a roughness factor which depends on the Young's Law contact angle determined by the surface chemistry. Because of the dependence of the liquid-air interface on the average distance between particles, the model appears to be very sensitive to the ε parameter (Figure 7).

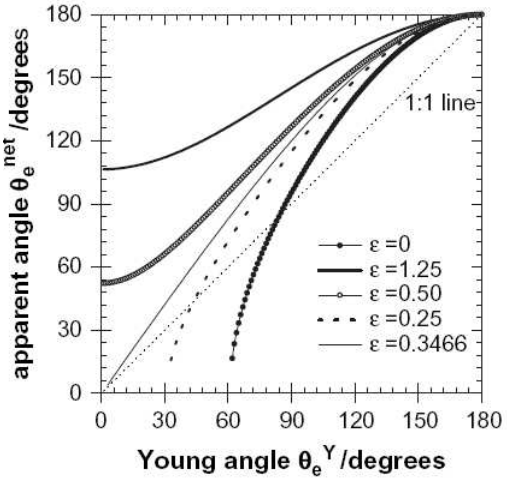

Figure 7 Effect of the combined Cassie-Baxter and Wenzel equation (Eq. 10) for the apparent equilibrium contact angle θ_e^{net} as a function of the the equilibrium contact angle, θ_e^Y for various average particle separations (ε).

When ε is greater than ~ 0.3, theory predicts an increase of the apparent equilibrium contact angle, θ_e^Y, for all Young's Law CAs from 0 to 180°. Calculation of the apparent CA for an interface between tape and water instead of air and water when the Young's CA is <90° produced slightly smaller CAs for the water-tape interface than those for air-water. In combination with small CAs measured for wettable particles adhering to the tape, which has an intrinsic CA of ~90°, this suggests that the tape does not introduce significant experimental artefacts. The validity of eq. 10 is lost when it predicts $\cos\theta_e^{net}$ >1; this corresponds with (a non-equilibrium) CA→0°, film formation and liquid penetration into the surface. The θ_e^{net} values depend on both the chemical nature of the surface and the local surface topography with the latter enhancing the effect of the former. This effect for a glass bead surface (Figure 3) is illustrated in Figure 8a.

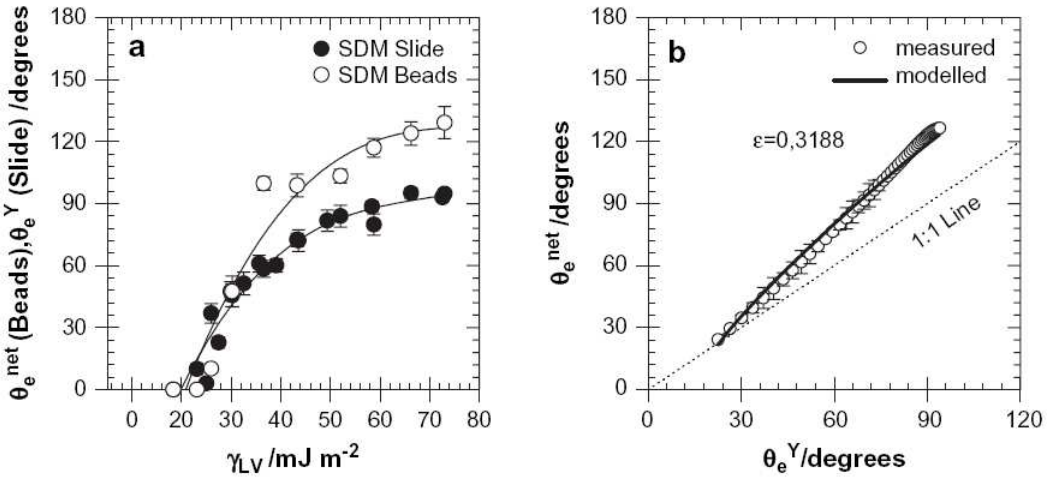

Figure 8 Sessile drop contact angles as a function of a liquid surface tension on a smooth hydrophobized glass plate and a layer of glass beads (a) and the relationship between contact angles for a layer of glass beads and those of a smooth glass surface obtained experimentally and predicted using Eq. 10 with ε = 0.319 (b).

The maximum CAs for the rough, repellent surfaces provided by silanized glass bead samples, 120°<CA<130° for γ_{LV} > 60 mJ m^{-2}, were larger than those of a smooth silanized glass surface (CA slightly >90°). At lower γ_{LV}, CAs for the beads fell close to, or below, those of the smooth glass surface. These data appear to be well described by 3rd order polynomials functions (Figure 8a). Using these polynomials to provide pairs of SDM-CA for beads (θ_e^{net}) with estimates of θ_e^{Y} made from the glass slide at various γ_{LV}, the predictions arising from the use of eq.10 show excellent agreement with experimental values, for glass beads exposed to 0.24 ml/100 g DCDMS, with the value of adjustable parameter ε=0.319 (Figure 8b). This clearly demonstrates the effect of the local topography on CAs. A value of ε= 0.302 was obtained by fitting data for the glass beads exposed to 0.12 ml/100 g DCDMS, suggesting that the model is reasonably stable with respect to ε for model particle systems. Values of ε obtained when this process was applied to polydisperse soils were found to be <0.3 (0.129 for clay soil, 0.295 for clay loam and 0.295 for sand, Figure 9).

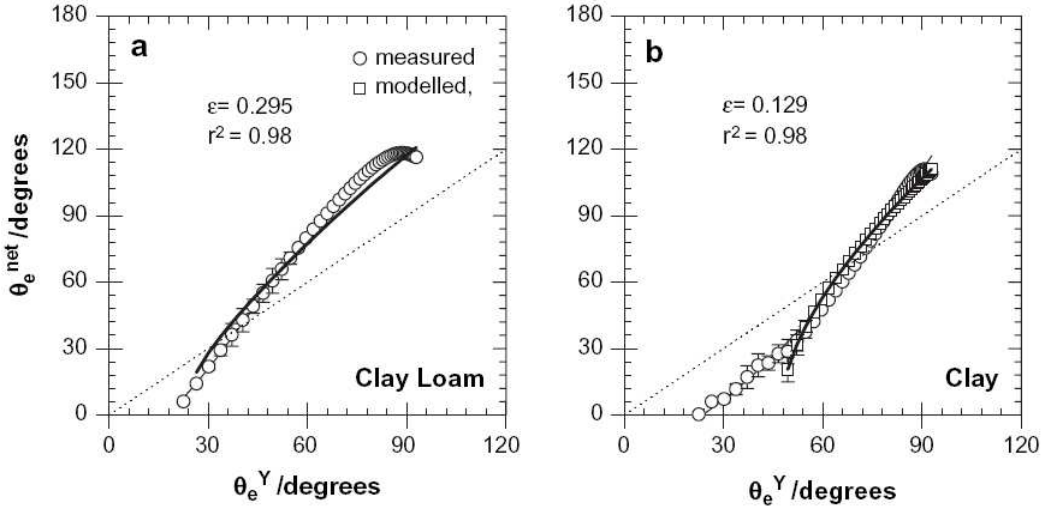

Figure 9: Experimentally determined contact angles for layers of particles of clay loam (a) and (b) (Clarinda) clay as a function of the corresponding CAs for smooth glass together with the values predicted with Equation 10.

These results indicate that the parameter ε is stable between 0.26 and 0.32, except for the clay samples. These also possess higher values of γ_C than the other samples, especially so at low doses of DCDMS (Tables 2 & 3):

Table 3: Critical surface energy γ_C as a function of the DCDMS dose. γ_C for smooth silanized glass is ~ 24 mJ m^{-2} (Zisman, 1964).

Soil	I*	II	III	IV	V
White Sand	33.0	27.0	26.2	25.7	24.3
Clay Loam	36.4	32.2	29.5	26.2	28.8
Clarinda Clay	57.5	43.8	32.4	32.2	34.0
Glass Beads	28.2	25.5	-	-	-

* DCDMS treatment see Table 2

Values of γ_C, deduced from average WPM-CA (θ_e^{net}) of beads, sand and loamy clay were similar to that of smooth silanized glass ($23 < \theta_e^Y < 26$ mJ m^{-2}). The smallest impact of surface roughness on θ_e^{net} as $f(\theta_e^Y)$ appeared to occur when ε was slightly below 0.347 (Figure 7) and appears to be consistent with estimates of γ_C (Table 3) made using Zisman's method (1964). Application of this method to data for the clay soil using, θ_e^{net} instead of θ_e^Y, led to enhanced values of γ_C as a consequence of generally smaller apparent CA (θ_e^{net}), a smaller average separation between its irregular particles and an insensitivity of γ_C to increasing doses of DCDMS. Values of θ_r for clay consistently ~0° indicate significant hysteresis in comparison with other samples (Figure 6) and suggest that a considerable proportion of the surface remains free from the influence of the highest dose of applied DCDMS. In addition, θ_r is susceptible to influence from any swelling of clay minerals following contact with aqueous media.

One highly uncertain parameter in the WPM-CA analysis is the estimate of the perimeter (Eq. 11) which in the simplest approximation is taken as the external dimensions of the plate. Buckton *et al*. (1995) estimated the effect of surface roughness on measured CA. By coating rough model surfaces with gold and then measuring the CA it was possible, because of the known surface energy of the model surface, to estimate the effective plate diameter. The CA measured on smooth gold-coated glass plates was found to be 68°, whereas for the rough surfaces an average angle of 49° was determined. It was concluded that the results on the rough surfaces were an underestimate of the true surface roughness. The minimum size of roughness which affects the contact angle was assumed to be smaller than 0.1 µm. Our relatively good agreement obtained between the (arithmetic) average WPM-CA and SDM-CA suggests that estimates of wetted perimeters based on macroscopic measurements, i.e. the macroscopic perimeter of the sample, were consistent with the effect of roughness on the CA of a sessile drop for the type of samples reported here.

Model predictions combining the influence of both surface chemistry and topography on rough layers of silanized, monodisperse particles appear to be accurate and precise to the variation ($0.26 < \varepsilon < 0.31$). The proposed model is generally able to predict the transition from smooth to rough and composite surfaces of various Wenzel roughness factors using a small number of simple assumptions about the surface topography.

CONCLUSIONS

To determine the contact angle of rough and irregular shaped surfaces we used the Wilhelmy Plate Method and the Sessile Drop Method which have previously (Bachmann *et al*., 2000; 2003) been adapted for soil particles. Application of a combination of the Cassie-Baxter and Wenzel equations to single layers of monodisperse spherical glass beads and to those of irregular soil particles, treated with DCDMS, produce reasonably accurate predictions of the CAs for a range of liquid surface tensions. Reference data, in the form of the Young´s law CAs, obtained from smooth DCDMS treated glass surfaces, account for the intrinsic surface chemical effects in the model. The only other parameter is the average separation between particles involved in the single layers. Estimates of critical surface energies made using Zisman´s method (Zisman, 1964) for both smooth glass and particle arrays suggest that surface topographies of these specimens do not affect the transition from an initial CA < 90° to 0° (complete wetting) to any significant extent. Combination of information from the

Wilhelmy plate and sessile drop methods shows promise in determining the initial wetting behaviour of air-dry irregularly shaped soil particles. The model and experimental data appear to be consistent for DCDMS treated surfaces in contact with aqueous ethanol solutions. Further work is required to adapt and establish the efficacy of these methods to naturally hydrophobic soils.

ACKNOWLEDGEMENTS

The authors are grateful to Prof. Robert Horton, Iowa State University, Ames, Iowa, USA for providing the three soil materials used for this study. We also acknowledge the assistance of Dr. Susanne Woche for the determination of the contact angles. We also thank two anonymous reviewers and the Associate Editor for their helpful remarks.

REFERENCES

Arye, G., Bachmann, J., Woche, S.K. & Chen, Y. 2006. Applicability of interfacial theories of surface tension to water-repellent soils. *Soil Science Society of America Journal*, **70**, 1417-1429.

Bachmann, J., Horton, R., & van der Ploeg, R.R. 2001. Isothermal and nonisothermal evaporation from four loamy sand soils of different water repellency. *Soil Science of America Journal*, **65**, 1599-1607.

Bachmann, J., Arye, G., Deurer , M., Woche, S.K., Horton, R. & Chen, Y. 2006. Universality of a surface tension – contact angle relation for hydrophobic soils of different texture. *Journal of Plant Nutrition & Soil Science-Zeitschrift fur Pflanzenernahrung und Bodenkunde*, **169**, 745-753.

Bachmann, J., Guggenberger, G., Baumgartl, T., Ellerbrock, R.H., Urbanek, E., Goebel, M.-O., Kaiser, K., Horn, R. & Fischer, W.R. 2008 Physical carbon sequestration mechanisms of soil organic matter under special consideration of soil wettability. Special Issue SPP 1090. *Journal of Plant Nutrition and Soil Science-Zeitschrift fur Pflanzenernahrung und Bodenkunde*, **171**, 14–26.

Bachmann, J., Horton, R., van der Ploeg, R.R. & S. Woche, 2000. Modified sessile drop method for assessing initial soil–water contact angle of sandy soil. *Soil Science of America Journal*, **64**, 564-567.

Bachmann, J., Woche, S.K., Göbel, M.-O., Kirkham, M.B. & Horton, R. 2003. Extended methodology for determining wetting properties of porous media. *Water Resources Research*, **39**, Art. 1353.

Buckton, G., Darcy, P. & McCarthy, D, 1995. The extent of errors associated with contact angles 3. The influence of surface roughness effects on angles measured using a Wilhelmy Plate Technique for powders, *Colloids and Surfaces A*, ***95***, 27-35.

Feng, L., Li, S.H., Li, Y.S., Li, H.J., L. Zhang, L.J., Zhai, J., Song, Y.L., Liu, B.Q., Jiang, L. & Zhu , D.B. 2002. Super-hydrophobic surfaces: From natural to artificial. *Advanced Materials*. **14**, 1857-1860.

Goebel, M.-O., Bachmann, J., Woche, S.K., Fischer, W.R. & Horton, R. 2004. Water repellency and aggregate size effects on contact angle and surface energy. *Soil Science Society of America Journal*, **68**, 383-393.

Good, R.J. 1993. Contact angle, wetting and adhesion: a critical review. In:. . *Contact angle, wettability and adhesion*. (ed K.L Mittal), Festschrift in honor of Professor R.J. Good. VSP, Utrecht, The Netherlands, pp 3-36.

Kamusewitz, H., Possart W. & Paul, D. 1999. The relation between Young's equilibrium contact angle and the hysteresis on rough paraffin wax surfaces. *Colloids and surfaces A: Physicochemical & Engineering Aspects*, **156**, 271-279.

Lavi, B., Marmur, A. & Bachmann, J. 2008. Porous media characterization by the two-liquid method: Effect of dynamic contact angle and inertia. *Langmuir*, **24**, 1918 –1923.

Marmur, A. 1994. Thermodynamic aspects of contact angle hysteresis. *Advances in Colloid & Interface Science*, **50**, 121-141.

Marmur, A. 2003. Kinetics of penetration into uniform porous media: testing the equivalent-capillary concept, *Langmuir*, **19,** 5956-5959.

McHale, G. 2007. Cassie and Wenzel: Were they really so wrong? *Langmuir*, **23**, 8200-8205.

McHale, G. & Newton, M.I. 2002. Frenkel´s method and the dynamic wetting of heterogeneous planar surfaces. *Colloids & Surfaces*, **A206**, 193-201.

McHale, G., Newton, M.I. & Shirtcliffe, N.J. 2005. Water-repellent soil and its relationship to granularity, surface roughness and hydrophobicity: a materials science view. *European Journal of Soil Science*, **56**, 445-452.

McHale, G., Shirtcliffe, N.J. & Newton, M.I. 2004. Super-hydrophobic and super-wetting surfaces: Analytical potential? *Analyst*, **129**, 284-287.

McHale, G., Shirtcliffe, N.J., Newton, M.I. & Pyatt, F.B. 2007. Implications of ideas on super-hydrophobicity for water repellent soil. *Hydrological Processes*, **21**, 2229-2238

Meiron, T.S., Marmur, A. & Saguy, I.S. 2004. Contact angle measurement on rough surfaces. *Journal of Colloid & Interface Science*, **274**, 637-644.

Neinhuis, C. & Barthlott, W. 1997. Characterization and distribution of water-repellent, self-cleaning plant surfaces. *Annals of Botany*, **79**, 667-677.

Roberts, F.J. & Carbon, B.A. 1972. Water repellence in sandy soils of South-Western Australia. II. Some chemical characteristics of the hydrophobic skins. *Australian Journal of Soil Research*, **10**, 35-42.

Siebold, A., Walliser, A., Nardin, M., Oppliger, M. & Schultz, J. 1997. Capillary rise for thermodynamic characterization of solid particle surface, *Journal of Colloid & Interface Science*, **186**, 60-70.

Spelt, J.K., Li, D. & Neumann, A.W. 1992. The equation of state approach to interfacial tensions. In: *Modern Approaches to Wettability: Theory and Applications*. (eds M.E. Schrader & G. Loeb), pp.101-142, Plenum Pres, New York.

Stange, M., Dreyer, M.E. & Rath, H.J. 2003. Capillary driven flow in circular cylindrical tubes. *Physics of Fluids*, **15**, 2587-2601.

Tschapek, M. 1984. Criteria for determining the hydrophilicity-hydrophobicity of soils. Z. Pflanzenernährung und Bodenkunde, **147**, 137-149.

Wilhelmy, L. 1863. Über die Abhängigkeit der Capillaritäts-Konstanten des Alkohols von Substanz und Gestalt des benetzten festen Körpers. *Annals of Physics*, **119**, 177-217.

Young, T. 1805. An essay on the cohesion of fluids. *Philosophical Transactions of the Royal Society of London*, **95**, 65-87.

Zisman, W.A. 1964. Relation of equilibrium contact angle to liquid and solid construction. In: *Contact Angle, Wettability and Adhesion*. (ed. R.F. Gould). Advances in Chemistry, Series **43**, 1-51. American Chemical Society, Washington, D.C.